Research Journal of Applied Sciences 11 (12): 1526-1533, 2016
ISSN: 1815-932X
© Medwell Journals, 2016

New Structure of III-V Tandem Solar Cells Based on Crystalline Silicon by using Trough Concentrator

Rached Ganouni, Mourad Talbi, Mohamed Fathi Boujmil and Hatem Ezzaouia
Center of Research and Technologies of Energy Borj-Cedria,Tunis,Tunisia

Abstract: Multi-junction Solar Cells (SC) made from III-V compound semiconductors are still in the development phase. Here, we perform calculations for multi-junction cells: GaInP and GaAs based on crystalline silicon (With band-gaps, respectively 1.85, 1.42 and 1.1eV) in order to obtain the optimal thickness and efficiency for each junction under the AM1.5 solar radiation spectrum. The ideal photo-current density is around 9.2 $mAcm^{-2}$ In order to reduce the problem of mismatch between cells and the tunnel junction costs and fabrication, we use a new structure of tandem solar cells in it we separates the cells in a good theoretical model. The expected conversion efficiency (η), under the AM1.5 spectrum (without tunnel junction), was determined to be around 46%, making this an attractive III-V compound tandem cell with crystalline silicon to be investigated in the near future.

Key words: GaInP/GaAs/c-Si, tandem solar cells, new structure, AM1, 5 illumination

INTRODUCTION

Multi-junction solar cells are regarded as photovoltaic devices which provide the most efficient way to convert solar energy to electric power. Currently these devices are widely used in space and terrestrial solar power facilities. Modern multi-junction monolithic GaInP/GaAs/Ge solar cells demonstrate total conversion efficiency over 30% under 1-sun illumination (Gnilenko and Plaksin, 2013).

Multi-junction (cascade or tandem) solar cells exploit so named spectrum separation principle (Luque and Hegedus, 2003). It is well known that single-junction solar cells can convert to electric power solar radiation with photon energy equal and above the semiconductor material band-gap. However, if the photon energy sufficiently exceeds the band-gap, excessive energy is lost to the lattice for heating instead of charge carrier generation. To achieve more conversion efficiency rate, several junctions of semiconductor materials with different band-gaps are stacked on top of one another decreasing the band-gap value from the top junction to the bottom one. This makes it possible to split solar energy spectrum into several sub-bands and to treat separately each sub-band with an appropriate semiconductor material. Each upper junction absorbs photons with energy higher than band-gap value but within only relatively narrow energy sub-band and allows all photons with lower energy to pass through it to the lower junction which can absorb photons with energy from next sub-band. The total spectral response and conversion efficiency of a multi-junction solar cell can be obtained as a sum of those characteristics of all individual junctions (subcells). There is no formal limitation to the number of subcells, but in practice increasing the number of junctions over four or five has no significant effect. The most used multi-junction solar cells consist of three junctions however, investigations towards involving more junctions to the solar cell design are in the progress. For instance the most important keys to highly efficient MJ solar cells are the abilities to: First, match current of all junctions at the optimal working condition (By using tunnel junction). Second match the lattice constant of all epitaxial layers to the substrate to achieve high crystalline quality (Yamaguchi, 2003).

In this study, we will introduce a new provision tandem solar cell by a model that will describe an innovation in the field of photovoltaic and avoiding the problems already announced. This model is based on a rigorous theoretical calculation using Matlab code (including optical and electrical modules). This study, focus on the design of a three junctions GaInP/GaAs/c-Si solar cell, under the standard AM1.5 solar spectrum, including the design of separation of cells and elimination of tunnel junction. Finally, we determined the reflectance, current density and efficiency of this new model.

Corresponding Author: Rached Ganouni, Center of Research and Technologies of Energy of Borj-Cedria,Tunis,Tunisia

MATERIALS AND METHODS

Theoretical approach: In this study, we propose a new model of GaInP/GaAs/Si-c tandem solar cell based on parabolic trough concentrator. This model is illustrated in Fig. 1. As shown in Fig. 1, this model is constitutes of three parabolic systems. The first, second and third parabolic system contains a single junction solar cells connected in series, respectively GaInP, GaAs and Si-c. Each of these solar cells is modeled in Fig. 2.

Each of GaInP, GaAs or Si-c cell is composed by absorbent layer TiO_2, p-n junction and reflective layer Al_2O_3 (Reflector (Al_2O_3+nSi (PECVD)) with 95% of reflexion) (Fig. 2a-c) GaInP single junction solar cells, GaAs single junction solar cells and Si-c single junction solar cells).

Where the thikness of each layer is named: x (TiO_2), x(Al_2O_3), x (n-material) = xj and x (p-material) = xB. The spectrum of sunlight striking the front of the cell includes ultraviolet, visible and infrared light. Sunlight is striking the GaInP cell, the absorption coefficient for short-wavelength light is quite large and most of blue light is absorbed very close to the front of GaInP cell. Light with energy close to, but above, the GaInP band edge is weakly reflected by the back surface of GaInP (contains a reflector Al_2O_3) throughout the cell and a large part reaches the GaAs cell. Light is reflected by the back surface of GaAs and absorbed by crystalline silicon. The study of our structure is based on the calculation of three fundamental terms. Reflectance R, external quantum efficiency QE and current density J.

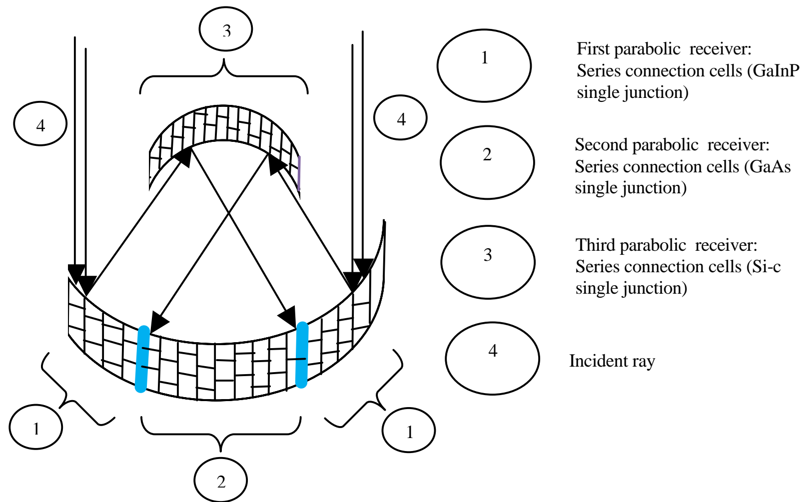

Fig. 1: New model of tandem solar cells with parabolic trough concentrator (In French: concentrateur cylindro-parabolique)

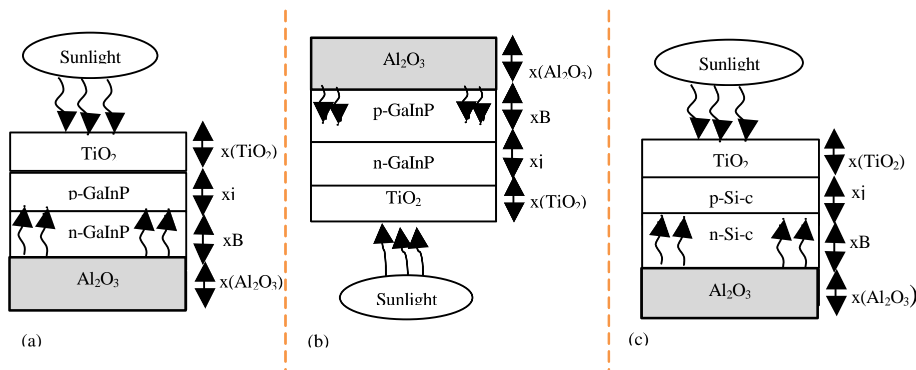

Fig. 2: Composition of GaInP, GaAs and c-Si solar cells: a) GaInP single junction cell; b) GaAs single junction cell; c) GaAs and c-Si cells

The optical modeling proposed in this study is based on the transfer matrix formalism. It allows calculation of the incident optical spectrum on each subcell from the solar cell spectrum. Each layer of the multi-junction is described by a transfer matrix M which is defined by:

$$M = \begin{pmatrix} m_{11} & m_{12} \\ m_{21} & m_{22} \end{pmatrix} = \begin{pmatrix} \cos(d_j) & \dfrac{i\sin(d_j)}{N_j} \\ iN_j\sin(d_j) & \cos(d_j) \end{pmatrix} \quad (1)$$

$$\delta_j = \frac{2\pi N_j}{\lambda} d_j \;; N_j = n_j(\lambda) + i\, k_j(\lambda)$$

where, $n_j(\lambda)$, $k_j(\lambda)$ and d_j are the refraction, extinction index and the thickness of the layer, respectively. The λ is the wavelength. The reflectance coefficient R (Bernal *et al*., 2015) of the layer is then given by:

$$R = |r|^2 = \left| \frac{(n_0 m_{1_1} + n_0 n_s m_{1_2} - m_{2_1} + n_s m_{2_2})}{(n_0 m_{1_1} + n_0 n_s m_{1_2} + m_{2_1} + n_s m_{2_2})} \right|^2 \quad (2)$$

Where:

n_0 = The superstrate refractive index
n_s = The substrate refractive index

The $m_{j,n}$ coefficients refer to the matrix transfer elements. Thus, it is possible to search the appropriate thickness of layer to calculate QE and J.

Multi-junction cells behave like homojunction cells in series, and their open circuit voltage is the sum of the voltages of the subcells while their short circuit is that of the subcell with the smallest current. Hence, the performance of a multi-junction cell can be obtained from the performance of each subcell evaluated independently. For each subcell, the load current density J is represented by the superposition of two diode currents and the photo-generated current:

$$J = J_p h - J_{01}\left(e^{qV/kT-1}\right) - j_{02}(e^{qV}/2^{kT}) - 1) \quad (3)$$

Where:

J_{ph} = The photocurrent density
J_{01} = The ideal dark saturation current component
J_{02} = The space charge non-ideal dark saturation current component

The photocurrent density is given by the sum of the photocurrents generated in the emitter, the base and the depleted region of the cell. Similarly, the dark current density is given by the sum of the dark currents generated in the emitter, the base and the depleted region of the cell (Fahrenbruch and Bube, 1983). We have:

$$J_{ph} = J_{emitter} + J_{base} + J_{depleted} \quad (4)$$

$$J_{emitter} = \frac{qF(1-R)\alpha L_p}{(\alpha L_p)^2 - 1} \times \begin{matrix} (S_pL_p)/D_p + \alpha L_p - e\left(-\alpha(x_j - W_n\right) \\ \left(S_pL_p\right)/D_p \cosh\left(x_j - W_n\right)/L_p + \\ \sinh\left[\left(\left(x_j - W_n\right)\right)/L_p\right]/ \\ \left(S_pL_p\right)/D_p \sinh\left[\left(x_j - W_n\right)/L_p\right] + co \end{matrix} \quad (5)$$

$$J_{base} = \frac{qF(1-R)\alpha L_p}{(\alpha L_n)^2 - 1} e - (x_B - w_n + w) \times \begin{cases} a L_{(n)} - \left(\left(S_nL_n\right)/D_n\right) \\ \left(\cosh\left[\left(x_B - W_p\right)/L_n\right]\right) - \\ e^{(-a(x_B - W_p))} + \sinh\left[\left(x_B - W_p\right)/L_{(n)}\right] \\ e^{(-a(x_B - w_p))}/(S_nL_n)/D_n \sin \end{cases} \quad (6)$$

$$J_{depleted} = q_F(1-R)e^{-a(x_j - W_n)}(1 - e^{-aW}) \quad (7)$$

$$J_{01} = J_{01,emitter} + J_{01,base} \quad (8)$$

$$J_{01,emitter} = q\frac{n_i^2}{N_D}\frac{D_p}{L_p}\left\{ \frac{\dfrac{S_pL_p}{D_p}\cosh[\dfrac{x_j - W_n}{L_p}] + \sinh[(x_j - W_n)/L_p]}{\dfrac{S_pL_p}{D_p}\sinh[(x_j - W_n)/L_p] + \cosh[(x_j - W_n)/L_p]} \right\} \quad (9)$$

$$J_{01,base} = q\frac{n_i^2}{N_A}\frac{D_n}{L_n}\left\{ \frac{\dfrac{S_nL_n}{D_n}\cosh[(x_B - W_p)/L_n] + \sinh[(x_B - W_p)/L_n])}{\dfrac{S_nL_n}{D_n}\sinh[(x_B - W_p)/L_n] + \cosh[(x_B - W_p)/L_n])} \right\} \quad (10)$$

$$J_{02} = \frac{Wn_i}{2(V_d - V)t} \quad (11)$$

Where:

q = The electron charge
F = The incident photon flux
α = The optical absorption coefficient
R = The reflectance of the anti-reflective coating
n_i = The intrinsic carrier concentration

N_A and N_D = The concentrations of acceptors and donors
X_j = The emitter thickness
X_B = The base thickness
L_p = The hole diffusion length in the emitter
L_n = The electron diffusion length in the base
S_p = The hole surface recombination velocity in the emitter
S_n = The electron surface recombination velocity in the base
D_p = The hole diffusion coefficient in the emitter
D_n = The electron diffusion coefficient in the base
τ = The non-radiative carrier lifetime
V_d = The build-in voltage of the junction, the thickness of the depleted layer in the emitter
W_n = The thickness of the depleted layer in the base
W_p = The total depleted zone thickness W (Wurfel, 2005) are given by:

$$V_d = kTLog\frac{N_D N_A}{n_i^2} \quad (12)$$

$$W = \sqrt{2e\frac{N_D + N_A}{N_D N_A}\left(V_d - V - 2kT\right)} \quad (13)$$

$$W_n = \frac{W}{\left(1+ {N_D}/{N_A}\right)} \quad (14)$$

$$W_p = W - W_n \quad (15)$$

Where:
k = The Boltzmann constant
ε = The dielectric constant
T = The temperature (T = 25°C was used in this study)

It is important to note that F and α depend on the wavelength whereas D_p, D_n, L_p, L_n and τ depend on the doping concentration. This model includes optical and electrical modules, with the optical modules allowing the research of the suitable thickness for each layer (x_j, x_B, x (TiO_2) and x (Al_2O_3)) of GaInP and GaAs. Then, the electrical model calculates the photocurrents in the space charge region, the emitter and the base for each junction.

Solar cell structure and parameters: The wavelength-dependent reflectance coefficient of GaInP and GaAs is based on the research of fitting curves of extinction $n_j(\lambda)$ and refractive $k_j(\lambda)$ index. The fit for this curves is given by Ghrib *et al*. (2011):

$$* n(\lambda)[GaInP] = 3.26 + \frac{8916.49}{4(\lambda - 408)^2} + 21609$$

$$* k(\lambda)[GaInP] = -0.0169 + \frac{34520}{4(\lambda - 334.2)^2} + 15672$$

$$* n(\lambda)[GaAs] = \frac{3.76}{1 + 1716.28e^{-(0.034\lambda)}};1$$

$$*k(\lambda)[GaAs] = \frac{3.39}{1 + e^{(\lambda - 474.45)} / 84.75}$$

$$*n(\lambda)[TiO_2] = 2.59 + 1.71e^{\{1-(\frac{\lambda-325.98}{38.99} - e^{\frac{-(\lambda-325.98)}{38.99}})\}}$$

$$k(\lambda)[TiO_2] = 1.167 - 1.162\left(\coth(\lambda - 336.26) - \frac{1}{\lambda - 336.26}\right)$$

$$*n(\lambda)[Al_2O_3] = 2.29623 + 1 + e\frac{0.17963}{\frac{(\lambda - 532.1490)}{35.08544}}$$

$$*k(\lambda)[Al_2O_3] = 0$$

$$*n(\lambda)\ [c - Si] = 3.31 + 9.46 * \exp(-0.0042\lambda)$$

$$*k(\lambda)\ [c - Si] = -0.074 + 263.54 * \exp(-0.0136 * \lambda)$$

The incident photon flux F for AM1.5 spectrum is taken by a fitting curve:

$$F = \frac{Ecl(\lambda)}{{hc}/{\lambda}} \quad (16)$$

$$Ecl(\lambda) = 0.06977 + 7.0625\left[1 - e\frac{-(\lambda - 0.26053)}{0.15994)})\right]^{2.28411} e\frac{-(\lambda - 0.26053)}{0.2285} \quad (17)$$

For 300 nm<λ<1400 nm. Where, Ecl (λ) (kW/m^2μm) the illumination, h Plancks constant, c velocity of light. The integrated ASTM Sub-commitee G3.09 AM1.5 solar spectral irradiance has been made to conform to the value of the solar constant accepted by the space community which is 694 W m^{-2}. The different parameters of GaAs, GaInP and c-Si are defined in Table 1-3. The non-radiative carrier lifetime are calculated

Table1: Values for the parameters of GaAs and GaInP (Kurtz *et al*. 1999) used in the model calculation

Parameters	GaAs	GaInP
Band gap Eg(ev)	1.42	1.86
The electron surface recombination velocity S_n (cm sec^{-1})	10^2	1.7 10^6
The hole surface recombination velocity S_p (cm sec^{-1})	10^6	10^4
Electron diffusion length L_n (μm)	25	3
Hole diffusion length L_p (μm)	0.1	0.5
Electron diffusion coefficient D_n (cm sec^{-1})	75	100
Hole diffusion coefficient D_p (cm sec^{-1})	1	5

Table 2: Values for the parameters (Schubert, 2006) of GaAs and GaInP used in the model

Parameters	GaAs	GaInP
Concentration of acceptors N_A (cm^{-3})	10^{18}	10^{18}
Concentration of donors N_D (cm^{-3})	10^{17}	10^{17}
Intrinsic carrier concentration (cm^{-3})	2.1×10^6	1.9×10^2
Permittivity	12.9	11.8

Table 3: Values for the parameters of c-Si used in the model calculation

Parameters	c-Si
Band gap Eg (ev)	1.1
The electron surface recombination velocity S_n (cm sec^{-1})	10?
The hole surface recombination velocity S_p (cm sec^{-1})	10^3
Electron diffusion length L_n (μm)	646
Hole diffusion length L_p (μm)	1.18
Electron diffusion coefficient D_n (cm sec^{-1})	41.8
Hole diffusion coefficient D_p (cm sec^{-1})	1.39
Concentration of acceptors N_A (cm^{-3})	2×10^{15}
Concentration of donors N_D (cm^{-3})	1.25×10^{19}
Intrinsic carrier concentration (cm^{-3})	4.29×10^{10}
Permittivity	11.8

according to the doping concentration by using empirical formulas summarized in Ghannam *et al*. (2004)'s research:

$$a_{GaInP} = 5.5\sqrt{E - E_g} + 1.5\sqrt{E - E_g - 1} \qquad (18)$$

The absorption coefficient of GaAs (Schubert, 2006) can be fitted by:

$$a_{GaAs} = 1.93\sqrt{E - E_g} \qquad (19)$$

The absorption coefficient of c-Si can be fitted by:

$$a_{c\text{-}Si} = 0.0312 + 0.00114 \times \exp(2.88E) \qquad (20)$$

Where:

E = The photon energy
E_g = The fundamental band gap, both in ev and α in 1 μ m^{-1}

RESULTS AND DISCUSSION

For each subcell when $\lambda<\lambda_{gap}$ the material must reflect the totality of photon but if $\lambda>\lambda_{gap}$ the material absorb the incident photon. According to this rule we modify the thickness of each subcell to obtain the suitable reflectance. Figure 3 shows the perfect

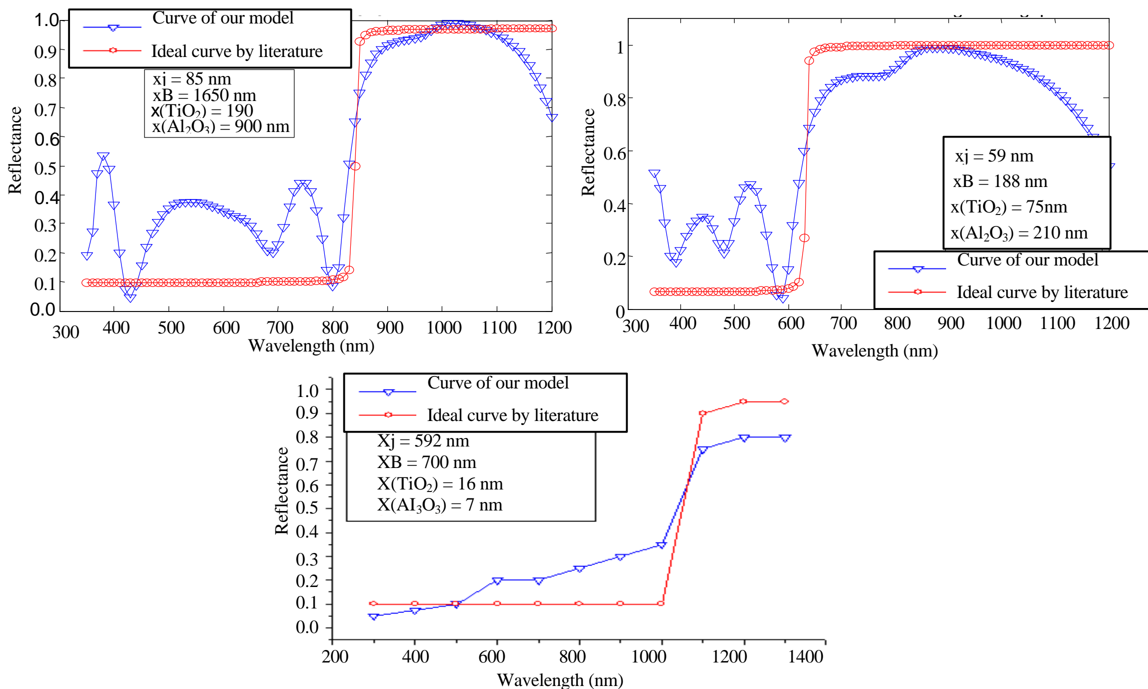

Fig. 3: The reflectance curve of: a) Reflactance GaAs the low bandgap cell; b) Reflactance GaInP the high bandgap cell; c) Reflactanceof c-Si

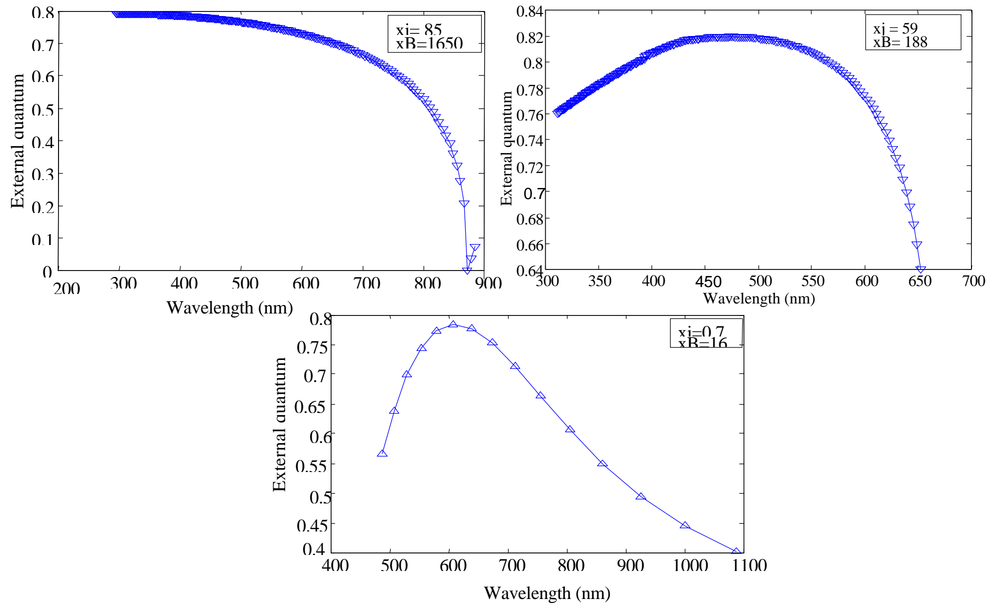

Fig. 4: The external quantum efficiency of: a) GaAs the low bandgap cell; b) GaInP the high bandgap cell; c) c-Si cell

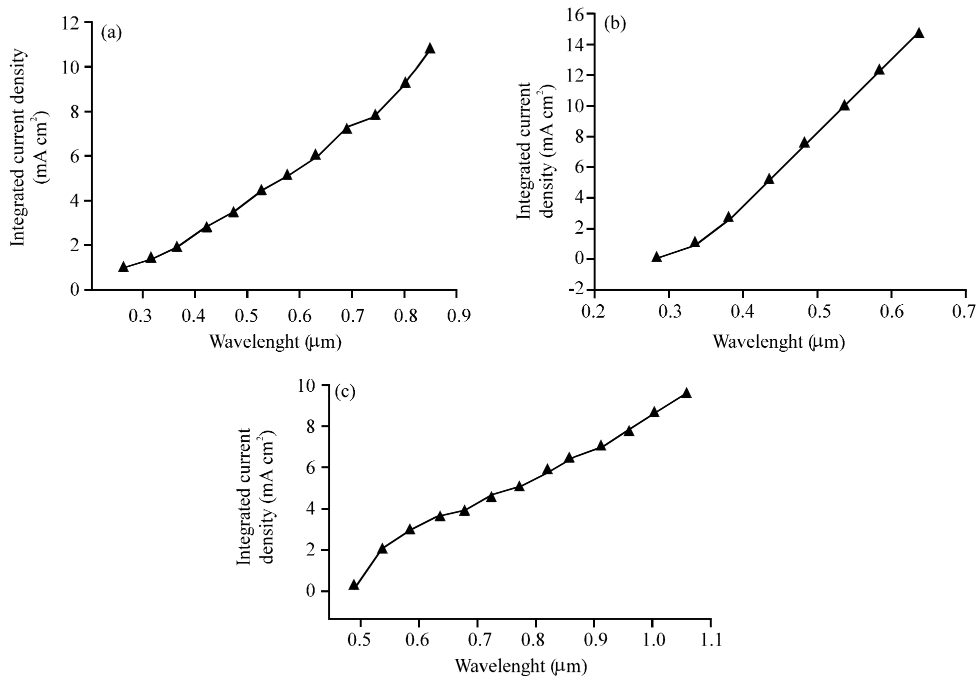

Fig. 5: Integrated photocurrent density of: a) GaAs the low bandgap cell; b) GaInP the high bandgap cell; c) Si-monocristallin

coherence between theoretical results and my simulation, thus the absorption of GaInP is important in the range of wavelength 300-650 nm whereas for GaAs is in the range of 300-850 nm and for c-Si is between 300-1100.

This result is very important to the next work, thus we can with the values of thickness X_j and X_B represent the curve of external quantum efficiency and density of current. Figures 4and 5 show the total external quantum

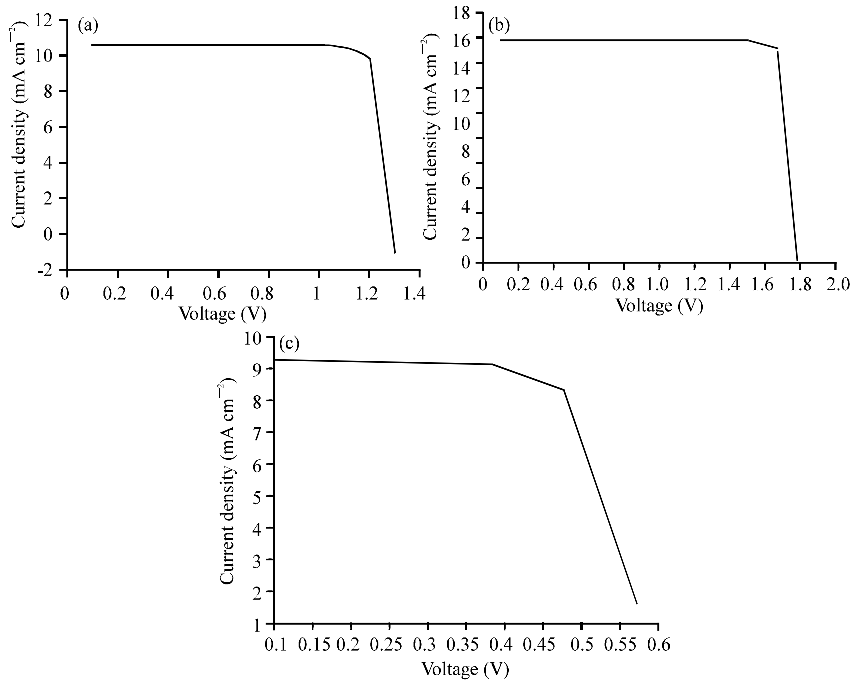

Fig. 6: I-V characteristics of GaInP, GaAs and c-Si under AM1.5: a) GaAs the low bandgap cell; b) GaInP the high bandgap cell; c) Si-monocristallin

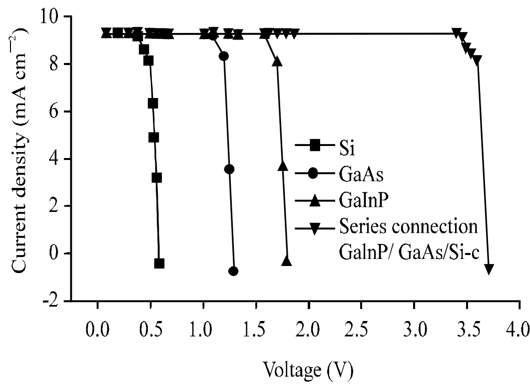

Fig. 7: I-V characteristics of the series connection between GaInP, GaAs and c-Si under AM1.5

efficiencies QE and the integrated photocurrent density J_{ph} of the two cells calculated from Eq. 4-7. The external quantum efficiency is a function of wavelength and the photocurrent density J_{ph} is obtained from the integral of the product of quantum efficiencies (We can use too this rule:

$$J_{ph} = \sum_{i=1}^{n} U_{ph}(\lambda_i)$$

The GaInP cell generates a photocurrent density of 16 mA cm^{-2}, the GaAs cell generates only 10 mA cm^{-2} and the last cell c-Si generates 9.2 mA cm^{-2}. Figure 6 show I-V characteristics for each subcell GaAs, GaInP and c-Si. For the case of a cell with the new structure without tunnel junction and with a serie connection between sub-cells, Jsc, Voc, FF and conversion efficiency η were determined for each of the junctions. Figure 7 shows the JBV curves for each of the sub-cells and the tandem cell in the new model.

Table 4: Calculated current densities, open circuit voltage, fill factor and power conversion efficiency for each of the sub-cells and for the full cell of new model model

Solar cell	Jsc (mA/cm^{-2})	Voc (V)	FF	η (%)
GaAs	9.2	1.300	87	14.9
GaInP	9.2	1.800	89	21.2
c-Si	9.2	0.585	83	6.40
Series connection model (GaInP with GaAs and c-Si)	9.2	3.685	94	46.0

J_{ph} (GaInP) = J_{ph} (GaAs) = J_{ph} (c-Si) = J_{ph} (Series connection model) = 9.2 mA cm^{-2}. The resultant JBV and is shown in Fig. 7. These results are summarized in Table 4. For the proposed tandem solar cell : Jsc = 9.2 mA cm^{-2}, Voc = 3.685V, FF = 0.94 and η = 46%. This is expected high conversion efficiency under the AM1.5 solar spectrum, comparable to current technology three junctions solar cells, and there for the GaInP/ GaAs/c-Si solar cell studied here is an attractive alternative for high efficiency solar energy conversion.

CONCLUSION

In this study, we have investigated theoretically the energy conversion efficiency that might be archived by GaInP/GaAs/c-Si mechanically stacked three-junction solar cell using optical model with parabolic trough concentrator. According to numerical simulation, we determined the optimized thickness o f GaInP, GaAs and c-Si. The optimal conversion efficiency was 46% which is higher than that of GaInP or GaAs single junction. Furthermore, the structure utilized in this work not only has high potential energy conversion efficiency, but also avoids the difficulties encountered in the technical difficulties of fabricating the tunnel junction and the costs. The calculations would contribute to designing and fabricating high efficiency GaInP/GaAs/c-Si mechanically stacked solar cell and this new structure can be a new research direction in GaInP/GaAs/c-Si three-junction solar cells.

REFERENCES

Bernal, C.R., M.A. Acevedo, A.P. Mora, J.M. Monsalve and M.L. Lopez, 2015. Design of Al x Ga 1-x As/GaAs/In y Ga 1-y As triple junction solar cells with anti-reflective coating. Mater. Sci. Semicond. Process., 37: 57-61.

Fahrenbruch, A.L. and R.H. Bube, 1983. Fundamentals of Solar Cells Photovoltaic Solar Energy Conversion. Academic Press, New York, USA.

Ghannam, M.Y., A.S. Alomar, N. Posthuma, G. Flammand and J. Poortmans, 2004. Optimization of the triple junction InGa0.5/GaAs/Ge monolithic tandem cell aimed for terrestrial applications using an experimentally verified analytical model. Kuwait J. Sci. Eng., 31: 203-234.

Ghrib, M., M. Gaidi, T. Ghrib, N. Khedher and M.B. Salam *et al*., 2011. Morphological and optical properties changes in nanocrystalline Si (nc-Si) deposited on porous aluminum nanostructures by plasma enhanced chemical vapor deposition for Solar energy applications. Appl. Surf. Sci., 257: 9129-9134.

Gnilenko, A.B. and S.V. Plaksin, 2013. Mechanically stacked triple-junction gainp gaas si solar cell simulation. J. Nano Electron. Physic., Vol. 5,

Kurtz, S.R., J.M. Olson, D.J. Friedman, J.F. Geisz and K.A. Bertness *et al*., 1999. Passivation of Interfaces in High-Efficiency Photovoltaic Devices. Vol. 573, Cambridge University Press, Cambridge, England, Pages: 95.

Luque, A. and S. Hegedus, 2003. Handbook of Photovoltaic Science and Engineering. 1st Edn., John Wiley and Sons, England.

Schubert, E.F., 2006. Absorption Coefficient of Various Semiconducting Materials, Light-Emitting Diodes. 2nd Edn., Cambridge University Press, Cambridge, England,.

Wurfel, P., 2005. Physics of Solar Cells: From Principles to New Concepts. Wiley-VCH, Berlin, Germany,.

Yamaguchi, M., 2003. III-V compound multi-junction solar cells: Present and future. Solar Energy Mater. Solar Cells, 75: 261-269.